Journal of Geoscience and Environment Protection, 2026, 14(4), 314-336
https://www.scirp.org/journal/gep
ISSN Online: 2327-4344
ISSN Print: 2327-4336

Comparative Study of Atmospheric Temperature Climate Trends over Central Africa Republic from Satellite and Reanalysis Data

Abdoul Nassir Silla[1,2*], Zhengkun Qin[1], Andrew Friday Hakabinga[1,3], Bakar Mohammed Yussuf[1], Tanimu Abubakar Sadiq[1,4]

[1]Key Laboratory of Meteorological Disaster of the Ministry of Education, International Joint Research Laboratory of Climate and Environment Change, Collaborative Innovative Centre on Forecast and Evaluation of Meteorological Disasters, School of Atmospheric Science, Nanjing University of Information Science and Technology (NUIST), Nanjing, China
[2]Faculty of Sciences, University of Bangui, Bangui, Central African Republic
[3]Zambia Meteorological Department Headquarters, Lusaka, Zambia
[4]Nigerian Meteorological Agency (NiMet), Nnamdi Azikiwe International Airport, Abuja, Nigeria
Email: *sillaabdoulnassir1@gmail.com

How to cite this paper: Silla, A. N., Qin, Z. K., Hakabinga, A. F., Yussuf, B. M., & Sadiq, T. A. (2026). Comparative Study of Atmospheric Temperature Climate Trends over Central Africa Republic from Satellite and Reanalysis Data. *Journal of Geoscience and Environment Protection, 14,* 314-336.
https://doi.org/10.4236/gep.2026.144017

Received: March 18, 2026
Accepted: April 25, 2026
Published: April 28, 2026

Abstract

Accurate and homogeneous long-term temperature records are essential for reliably estimating the rate of global warming and informing appropriate adaptation strategies. However, the Central African Republic (CAR) is characterized by an extremely sparse and irregular network of meteorological observations, which severely hampers the nation's ability to assess and respond to climate-related hazards. To better estimate atmospheric warming rates over CAR and evaluate the applicability of reanalysis products in this region, this study conducts a systematic comparative analysis of atmospheric temperature trends using satellite-based observations from the Advanced Microwave Sounding Unit-A (AMSU-A) during 2000-2020, in conjunction with three state-of-the-art reanalysis products: ERA5, JRA-55, and MERRA-2. Linear and nonlinear trend analyses are performed on regionally averaged temperature anomalies at three pressure levels (500, 250, and 100 hPa). All datasets reveal statistically significant warming in the troposphere and lower stratosphere. The satellite-derived warming rates over CAR are 0.576, 0.243, and 0.324˚C/decade at the three levels, respectively, which are generally larger than those from the reanalysis products. The brightness temperature trends show better agreement with reanalysis data at 500 hPa and 100 hPa, whereas substantial discrepancies are evident at 250 hPa in the transition zone. The differences in nonlinear

trends are even more pronounced: the satellite observations exhibit distinct nonlinear warming characteristics, whereas all reanalysis products demonstrate approximately linear trends. Inter-comparison among the reanalysis products indicates notable discrepancies in temperature trends, with differences exceeding a factor of two in the lower troposphere. Among the three reanalysis products, ERA5 shows the closest agreement with satellite observations, suggesting its superior regional applicability over CAR. The trends in the brightness temperature show the best agreement with the reanalysis data at 500 hPa, as the inter-dataset spread is small. Moderate agreement is seen at 100 hPa, while the highest discrepancies are seen at 250 hPa, as the AMSU-A channel 7 weighting function overlaps the tropical tropopause layer.

Keywords

Air Temperature, Climate Trend, Nonlinear Trend, AMSU-A, Reanalysis

1. Introduction

The Central African Republic (CAR) is a landlocked country located in the heart of central Africa, characterized by predominantly tropical climate and strong dependence of livelihoods on climate sensitive natural resources. In the Central African Republic, climate variability exerts a strong influence on key socio-economic sectors, particularly agriculture, public health, urban planning, and human thermal (Ngoma et al., 2021; Ogunrinde et al., 2019). Variations in air temperature affect crop growth cycles, soil moisture conditions, and evapotranspiration rates, thereby influencing agricultural productivity and food security.

As an equatorial region perennially affected by extreme heat, air temperature is one of the most essential climatic variables for understanding climate and their impacts on natural and human systems. Rising temperatures also intensify heat stress and contribute to the spread of climate sensitive diseases, while increasing cooling demands in urban areas and reducing overall thermal comfort for populations. Several studies have demonstrated that variations in air temperature directly influence agricultural productivity, building design, and overall quality of life in both urban and rural environments across Central Africa (Ndiaye et al., 2020).

Recent changes in air temperature must be interpreted within the broader context of global climate warming. At the global scale, rising mean temperature are primarily attributed to increasing anthropogenic greenhouse gas emissions (Legg, 2021). In Africa, this warming trend is particularly pronounced, with observed temperature increases often exceeding the global average, resulting in more frequent and intense heatwaves, elevated thermal stress (Dosio et al., 2018; Harrington et al., 2016; Nangombe et al., 2019). Numerous studies have further shown that global warming levels of 1.5˚C, 2˚C, and 3˚C are associated with substantial shifts in temperature and precipitation regin-me across the African continent, in-

cluding Central Africa (Dosio et al., 2021).

Climate research in Africa has advanced considerably over recent decades. Numerous studies have investigated variability and long-term trends in temperature and precipitation at continental and regional scales, highlighting the pronounced spatial heterogeneity of African climate (Funk et al., 2019). In Central Africa, several investigations have focused on detecting climate change signals, assessing historical and recent climate evolution, and evaluating sectoral impacts, particularly with respect to agricultural, human health and water resources (Fotso, 2022; Sylla et al., 2016; Washington, 2020).

Reliable climate datasets constitute the foundation of climate variability and trend analysis, as the detection of climate change signals strongly depends on data length, and Mudelsee (2019). Long time series are essential for detecting climate change signals and for distinguishing anthropogenic trends from natural climate variability (Rohde et al., 2016; Vincent et al., 2012). Consistent data availability is also crucial for informing climate adaptation strategies and risk management policies, particularly in vulnerable regions of Central Africa (Saber et al., 2025). The integration of multiple independent datasets further enhances confidence in trend estimates and helps to quantify observational uncertainties.

One of the major challenges for climate research in the CAR is the very limited number of operational meteorological stations and the discontinuity of available ground based observational records (Dinku, 2019; Hua et al., 2019). This weak observational network significantly hampers detailed long term climate trend analyses and restricts the ability to accurately assess spatial and temporal variability in air temperature at both local and national scales. These have examined, among other aspects, the influence of climate variability on malaria transmission in Bangui (Nzoumbou-Boko et al., 2022) impacts on agricultural production (Mbétid-Bessane et al., 2010), and adaptation strategies adopted by rural communities in response to climate change (Abaje et al., 2016), however the scope and robustness of these studies remain constrained by the scarcity of local climate observations.

Given these constraints, access to reliable homogeneous, and long-term climate datasets has become a critical issue for climate trend analysis. In response to this observational gap, satellite observations and reanalysis products have become indispensable alternatives to *in situ* measurement. These datasets have been widely used to investigate air temperature trends, precipitation variability, and extreme climate events during the satellite era (Adler et al., 2017; Hersbach et al., 2020). In Central Africa, such approaches have substantially improved understanding of regional climate variability and change, particularly with respect to temperature trend, precipitation patterns, and climate regionalization (Almazroui et al., 2021), although uncertainties persist due to limited ground-based validation data.

Within this framework, the present study aims to analyze air temperature variability and trends in the Central African Republic using satellite derived observations and reanalysis datasets. The objective is to better characterize recent climate

evolution in this poorly instrumented country, identify robust climate change signals, also provide valuable guidance for the application of reanalysis products in climate research over the CAR region.

2. Data and Methods

2.1. Study Area and Climatic Context

The Central African Republic is a landlocked country located between approximately 2˚N-11˚N and 14˚E-27˚E in the heart of Central Africa (Figure 1). The topographic height over Central African Republic is also shown in Figure 1. The CAR region is predominantly characterized by plains, with two elevated terrain areas located on its eastern and western flanks. The climate is characterized by two dominant seasons: a dry season (November-March) and a rainy season (April-October). The seasonal cycle is governed primarily by the north-south migration of the Intertropical Convergence Zone (ICTZ). During the dry season, reduced cloud cover and rainfall promote stronger surface heating, particularly in the northern regions. During the rainy season, enhanced cloudiness and deep convection lad to more homogeneous temperature distributions.

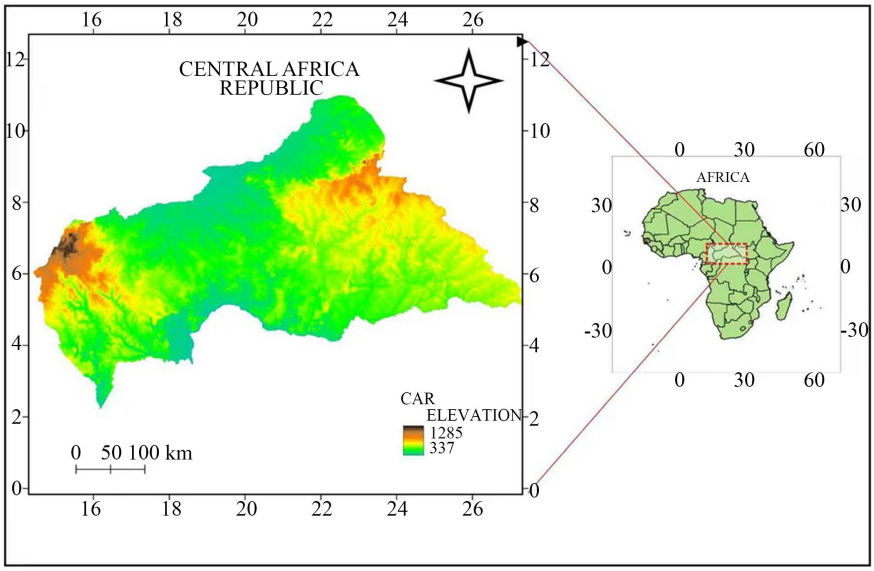

Figure 1. Spatial distribution of topographic height over Central African Republic, showing the study area.

2.2. Data

2.2.1. Satellite Derived Temperature Data (AMSU-A)

The satellite-derived atmospheric temperature data used in the present study is obtained from the Advanced Microwave Sounding Unit-A (AMSU-A) instruments flown on the series of polar-orbiting satellites from the National Oceanic and Atmospheric Administration (NOAA). AMSU-A is a passive microwave radiometer that is designed to measure the thermal emission from atmospheric oxygen absorption bands at 50 - 60 GHz frequency ranges, thus providing vertically

weighted atmospheric temperature profiles in the troposphere and lower stratosphere (Weng et al., 2005). It consists of 15 channels of microwaves with frequency ranges between 23.8 and 89 GHz.

AMSU-A instruments have flown on several polar-orbiting satellites from the NOAA series, including NOAA-15, NOAA-16, NOAA-17, NOAA-18, NOAA-19, as well as the European Space Agency's MetOp-A, MetOp-B, and MetOp-C satellites since 1998, thus providing a long-term global atmospheric temperature data set (Ferraro et al., 2018). It has a swath width of 1650 km with a nadir spatial resolution of 40 - 50 km. Satellite data from AMSU-A are also useful in climate studies in the Central African Republic (CAR), where there are extremely limited data from ground-based meteorological stations. For data-scarce regions, satellite data are useful in providing spatially continuous data on the variability and trends in atmospheric temperature. However, it should be noted that there are various sources of uncertainty in using data from AMSU-A. For example, there are concerns related to surface emissivity, effects of clouds and precipitation, and those related to the retrieval of atmospheric temperature using microwave radiances (Mears & Wentz, 2009). To mitigate potential contamination from complex surface conditions, this investigation restricts attention to AMSU-A channels 5, 7, and 9, with weighting function maxima near 500 hPa, 250 hPa, and 100 hPa, respectively. Consequently, the observed brightness temperatures are indicative of atmospheric temperatures at these respective levels.

It should also be noted that AMSU-A makes use of a cross-scan approach in collecting data, where a change in scan angle varies the field of view of the instrument. While it has a spatial resolution of 50 km at nadir points, it reduces to almost 200 km at the extremes of the scan swath. There are also differences in various instruments flown on successive satellites, where calibration biases and orbital drift are also concerns (Mears & Wentz, 2009). For climate studies to be consistent, several studies have established homogenized temperature data sets from the AMSU-A satellite-based brightness temperatures. This has been done through the inter-satellite calibration techniques to produce long-term stable atmospheric temperatures for climate trend analysis (Mears & Wentz, 2009; Quénol, 2011).

The present study utilizes the AMSU-A gridded climate dataset developed by (Qin & Zou, 2023). The AMSU-A gridded atmospheric temperature dataset is created using a step-by-step process that includes calibrating the measurements, checking for quality issues, correcting for diurnal variation, adjusting for differences between satellites, removing cloud effects, and building layers of temperature data using specific channel weights. Brightness temperature data from different NOAA satellites are matched during times when they overlap to make sure the data stays consistent over time (Qin & Zou, 2023). Then, monthly average temperatures are put on a regular grid and averaged across regions to create time series. This helps reduce sudden changes and lowers errors caused by satellite movement or switching between satellites. Testing has shown that the AMSU-A dataset gives a good picture of how the atmosphere's temperature changes over

time and shows long-term trends (Qin & Zou, 2023). Comparing it with radiosonde data and modern climate models shows that they agree well in the middle and upper parts of the atmosphere.

As CAR is situated predominantly over land, this study focuses on AMSU-A channel 5 and channels with higher-peaking weighting functions to minimize the influence of uncertainties in surface emissivity. **Table 1** provides the pressure levels corresponding to the peaks of the weighting functions for each channel. The analysis period spans January 2000 to December 2020. While the AMSU-A channels actually measure vertically weighted brightness temperatures, the reanalysis data provide air temperatures at specific pressure levels. As a result, the two are physically different quantities, and any numerical comparison between the two is therefore necessarily approximate. To help mitigate this problem, the reanalysis temperature profiles were convolved with the appropriate AMSU-A weighting functions to produce synthetic brightness temperatures, prior to the calculation of trends, with the differences between the original and synthetic data being recognised as a systematic uncertainty, as discussed in Section 7.

2.2.2. Reanalysis Datasets

Global reanalysis products represent another category of regularly gridded long-term datasets suitable for climate research. Employing sophisticated numerical models, these products utilize model simulations as background fields and incorporate as many reliable observations as possible through data assimilation techniques to generate analysis fields that are statistically optimal estimates of the true state. While continuously refining their numerical weather prediction models, numerous countries have developed their own global reanalysis datasets. To ensure the generality of our findings, three reanalysis products developed by different institutions are selected herein: ERA5, JRA-55, AND MERAA-2.

ERA5 (ECMWF 5th Generation Atmospheric Reanalysis) is the fifth generation atmospheric reanalysis produced by the European Center for Medium Range Weather Forecasts (ECMWF). ERA5 is generated using the Integrated Forecasting System (IFS) and a four-dimensional variation (4D-VAR) data assimilation scheme. It provides globally consistent atmospheric, land, and ocean variables at an hourly temporal resolution and a native horizontal resolution of approximately 31 km, with 137 vertical levels extending from the surface to 0.01 hPa. ERA5 covers the period from 1940 to the present and assimilates a wide range of satellite and *in situ* observations, offering substantial improvements over earlier ECMWF reanalysis in terms of spatial resolution, temporal continuity, and representation of physical processes (Hersbach et al., 2020)

MERRA-2 (Modern-Era Retrospective analysis for Research and Applications, Version 2) is produced by NASA's Global Modeling an Assimilation Office using Goddard Earth Observing system Model, Version 5 (GEOS-5), and an incremental analysis update assimilation scheme. MERRA-2 covers the period from 1980 to the present and has a native horizontal resolution of approximately $0.5^{\circ} \times 0.625^{\circ}$, with 72 vertical levels extending from surface to 0.01 hPa. A distinctive

feature of MERRA-2 is its explicit assimilation of aerosol observations, with improves the representation of radiative processes and their influence on atmospheric temperature (Gelaro et al., 2017).

JRA-55 (The Japanese 55-year Reanalysis) is produced by the Japan meteorological Agency using a state-of-the-art global spectral model and four-dimensional variations data assimilation system. JRA-55 spans the period from 1958 to the present and is provided at a horizontal resolution of approximately 55 km with 60 vertical levels. A key strength of JRA-55 is the consistent assimilation of historical satellite observations using modern retrieval algorithms, which improves temporal homogeneity across the entire record. JRA-55 has demonstrated good performance in representing large scale atmospheric circulation and temperature variability, particularly in the free troposphere (Kobayashi et al., 2015).

For each reanalysis dataset, monthly mean air temperature fields at standard pressure levels (100, 250, and 500 hPa) were extracted for the Central African Republic domain. To ensure inter dataset consistency, all data were interpolated onto a common regular grid of 0.5˚ × 0.5˚. The CAR domain is given by the geographic mask 14˚E-27˚E, 2˚N-11˚N, with the restriction that only land points are considered. The bilinear interpolation brings all the data to the common 0.5˚ grid. The area-weighted spatial averaging uses cosine latitude weighting. Months with less than 20 valid data points are set to missing and not interpolated. Less than 0.5% of the data points are set to missing in any of the data sets over the period 2000-2020.

Spatial averaging was then applied to generate regional mean time series for each pressure level and dataset.

2.3. Climate Trend Calculation Methods

To ensure methodological transparency and reproducibility, this section explicitly presents the mathematical formulations used for linear and nonlinear trend estimation.

2.3.1. Temperature Anomalies

Monthly temperature anomalies are calculated by removing the mean seasonal cycle from the original temperature time series. Let $T_m(y)$ denote the monthly mean air temperature for month m in year y. The climatological mean for month mean over the analysis period is defined as:

$$T_m = \frac{1}{N}\sum_{y=1}^{N} T_m(y),$$

where N is the total number of years in the study period (2000-2020). The temperature anomaly is then computed as:

$$T' = T_b - T_m$$

2.3.2. Seasonal Averaging

Seasonal mean temperature anomalies are computed by averaging monthly anomalies over the two dominant climatic seasons of the Central African Republic: the

dry season and the rainy season. For a given season *s*, consisting of M_s months, the seasonal anomaly is defined as:

$$T_s'(y) = \frac{1}{M_s} \sum_{m \in s} T'(m, y)$$

This approach explicitly reflects the bimodal seasonal structure of the CAR climate and avoids the use of boreal-standard seasons (e.g., DJF, JJA), which are not physically representative of the region.

2.3.3. Linear Trend Estimation

Let $T(t)$ denote the monthly mean air temperature anomaly at time t, where $t = 1, 2, \cdots, N$ resents the time index in months overs the study period (2000-2020). The linear trend is estimated using ordinary least squares regression.

$$T(t) = \alpha + \beta(t) + \varepsilon,$$

where α is the intercept, $\beta(t)$ is the linear trend coefficient (˚C month^{-1}) and ε is the residual term representing internal climate variability and observational noise. The statistical significance of the trends can be evaluated by a two-tailed Student's t-test. Serial autocorrelation is addressed by using the effective sample size $N_{eff} = N(1-r)/(1+r)$, where r is the lag-1 autocorrelation of the OLS residuals. The standard error is multiplied by $\sqrt{N/N_{eff}}$ prior to the calculation of confidence intervals. All trends in **Table 1** are statistically significant at $p < 0.05$ after this correction.

2.3.4. Nonlinear Trend Estimation Using Ensemble Empirical Mode Decomposition (EEMD)

To better understand the mechanisms driving climate warming, we need more than just average warming rates, we also need to look at how those rates change over time. Linear trend analysis gives a basic idea of long-term changes, but it assumes the warming rate stays the same, which isn't always true. This means it can miss periods when warming speeds up, slows down, or even shifts in a big way. More and more, scientists are seeing that warming in the atmosphere, especially over land, doesn't follow a straight path. It can change because of factors like shifts in heat absorption, interactions between land and air, and natural climate swings (Qin & Zou, 2023). Spotting these changes is especially important in places like the Central African Republic, where faster warming could make heat worse, hurt farming, and damage ecosystems.

To characterize time varying and nonlinear temperature, this study applies the Ensemble Empirical Mode Decomposition (EEMD) technique to monthly temperature anomaly time series, following the methodology of (Qin & Zou, 2023). The only authoritative EEMD parameters used throughout the study are as follows: The number of ensemble members = 100, the amplitude of the white noise = 0.2 × σ of the original series, and the standard EMD stopping criterion of "residual monotone or <= 1 extremum" as recommended by Wu et al. (2011) and consistent with the findings of Qin & Zou (2023). The erroneous sentence stating 400 ensemble members has been

deleted EEMD is an adaptive, data driven decomposition method designed to separate non stationary and nonlinear signals into physically meaningful components without prescribing any basis functions.

Given a temperature anomaly time series $T(t)$, it is decomposed as

$$T(t)=\sum_{k=1}^{k} C_k(t)+R(t)$$

where $\left(C_k(t)\right)$ denotes the intrinsic mode functions (IMFs) representing oscillatory components from high to low frequency, and $\left(R(t)\right)$ is the residual component representing the nonlinear trend.

The decomposition proceeds iteratively as follows:

1) Identify all local maxima and minima of the current residual $\left(R_{k-1}(t)\right)$.

2) Construct upper and lower envelopes using cubic spline interpolation.

3) Compute the local mean $m_k(t)$ of the two envelopes.

4) Extract the IMF:

$$C_k(t)=R_{k-1}(t)-m_k(t)$$

5) Update the residual:

$$R_k(t)=R_{k-1}(t)-C_k(t)$$

The EEMD decomposition process will continue in an iterative manner until the residual is either a monotonic function or has at most one extremum, to ensure that there are no more oscillatory components that can be extracted. In this research, the EEMD algorithm was carried out with 100 ensemble members, with the amplitude of the added white noise set to 0.2 times the standard deviation of the original time series, as suggested by (Wu et al., 2011). For each ensemble member, the intrinsic mode functions (IMFs) were extracted in a sequential manner, and the ensemble mean of the corresponding IMFs was computed to remove mode mixing caused by noise.

After removing the first $k=13$ IMFs representing oscillatory components from high to low frequency. The EEMD decomposition was performed with 400 ensemble members and a noise amplitude of 0.2 times the standard deviation of the input series, with 10 sifting iterations per IMF.

$$T_{nl}(t)=R_k(t)$$

3. Seasonal Climatology of Air Temperature

Seasonal climatology is examined for the dry season and rainy season, based on multi-year averages over 2000-2020. These two seasons represent the dominant climatic modes of the Central African Republic and are defined according to the annual north-south migration of the Intertropical convergence Zone (ITCZ) which control regional rainfall, cloud cover, and convective activity. This seasonal partitioning better reflects the physical climate system of the region than the use of standard boreal seasons and allows a more meaningful interpretation of temperature variability in relation to regional atmospheric processes.

3.1. Dry Season Climatology

During the dry season, i.e., from November to March, the temperature of the atmosphere in the CAR is determined by the combined effects of diminished cloudiness, weakened convection, and enhanced surface heating resulting from the southward shift of the Intertropical Convergence Zone (ITCZ). As the sky is clear, solar insolation is enhanced, resulting in an increase in sensible heat flux, especially over the northern savanna regions, where the vegetation cover is meager. On the other hand, surface heating is moderated in the southern part of the CAR, where the tropical forest is denser, along with enhanced evapotranspiration.

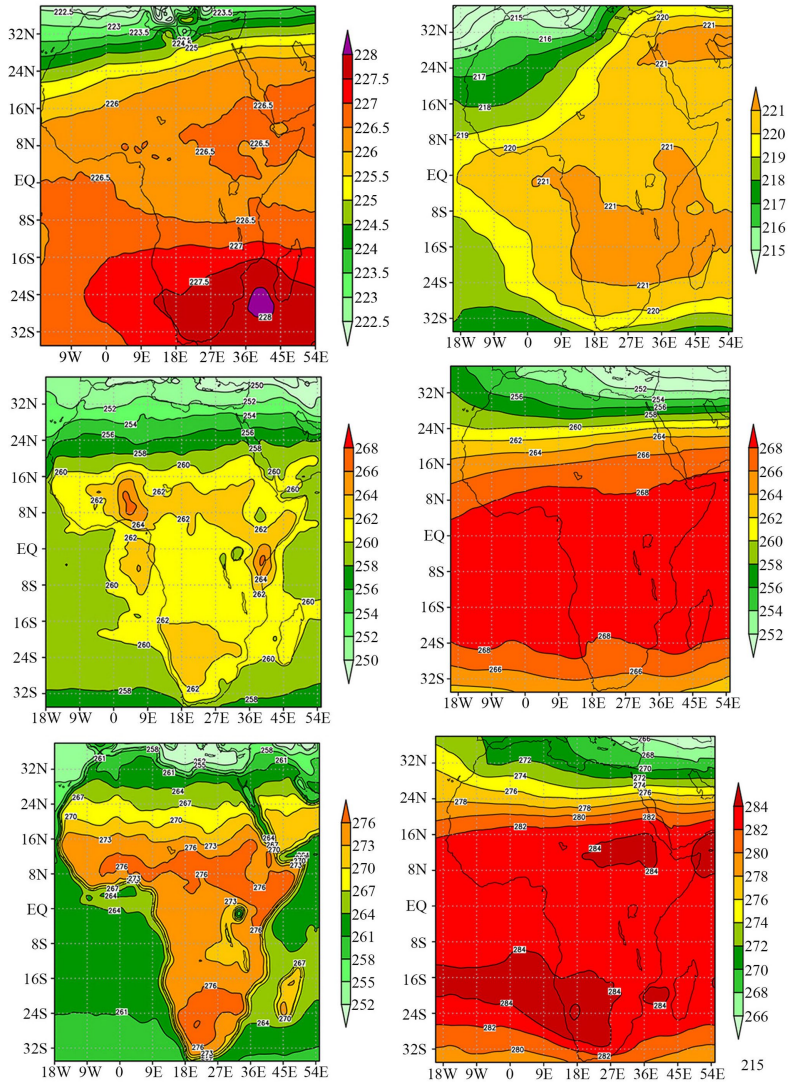

Figure 2. Spatial distribution of temperature at 100, 250, and 500 hPa for satellite data (left panels) and ERA5 (right panels) on dry season.

Figure 2 presents the spatial distributions of temperature at various levels over Africa during the dry season across different datasets. As precipitation effects are minimal during the dry season, temperatures exhibit predominantly zonal patterns,

with extensive high-temperature regions covering the equatorial zone. The dry season shows a meridional temperature gradient characterized by lower temperatures in the north and higher temperatures in the south, indicating that temperature at these altitudes is primarily determined by insolation. Although the spatial structures are broadly similar among the different datasets, discrepancies exist in the location of high-temperature regions; At 100 hPa, the AMSU-A data show an additional high-temperature center in the southern part of the region. In the lower troposphere, although the AMSU-A data can also well reproduce the meridional temperature gradient, the land-sea thermal contrast is relatively pronounced.

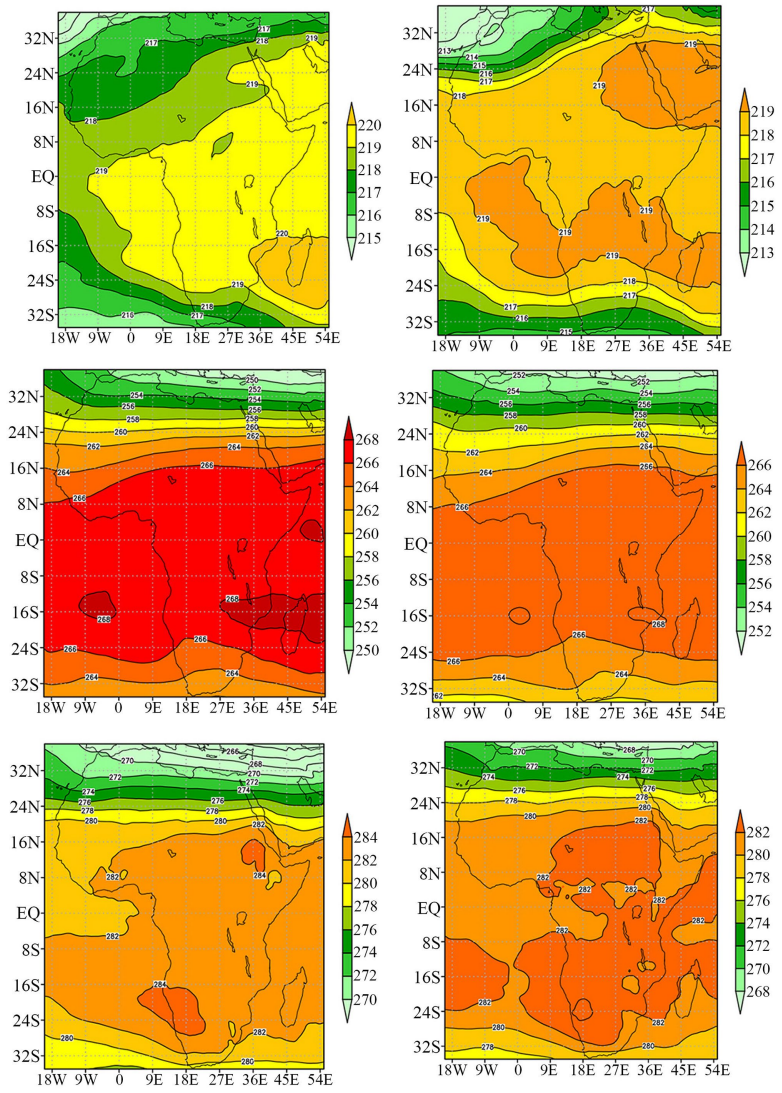

Figure 3. Spatial distribution of temperature at 100, 250, and 500 hPa for JRA-55 (left panels) and MERRA-2 (right panels) on dry season.

Differences in spatial structure are also evident among the reanalysis products (**Figure 3**). At 100 hPa, JRA-55 exhibits a distinctly different warm region compared to the other two reanalysis datasets, resembling more closely the AMSU-A

data, with the maximum temperature occurring in the northern part of the region, whereas ERA5 and MERRA-2 center their warm anomalies over the tropics. At 500 hPa, ERA5 displays a more pronounced zonal temperature distribution, while JRA-55 and MERRA-2 show two extrema on either side of the equator, a pattern more consistent with the satellite observations.

3.2. Rainy Season Climatology

During the rainy season (April-October), the northward migration of the Intertropical Convergence Zone (ITCZ) intensifies cloud cover, deep convection, and strong-scale moisture convergence in the Central African Republic (CAR). More cloud cover reduces the surface net shortwave radiation because of increased cloudiness, and latent heating from convection also modifies the vertical temperature profile. As a result, the horizontal temperature gradients are reduced and the spatial homogeneity of the atmospheric temperature field is increased compared to the dry season.

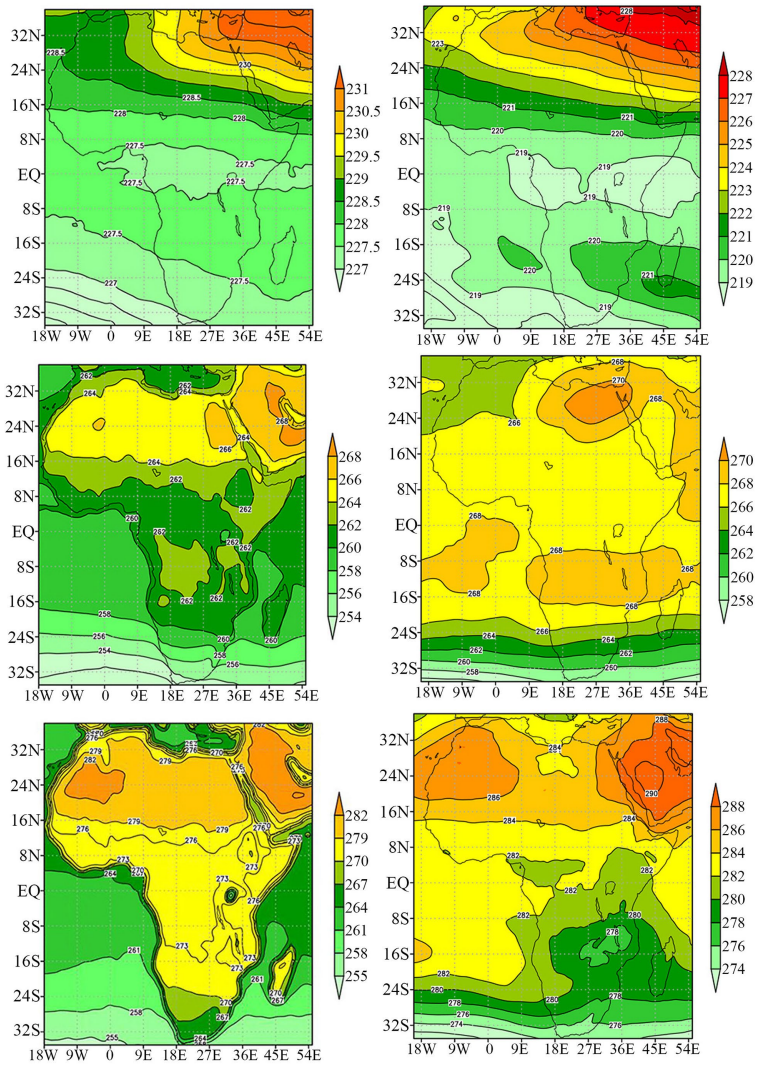

Figure 4. Spatial distribution of temperature at 100, 250, and 500 hPa for satellite data (left panels) and ERA5 (right panels) on rain season.

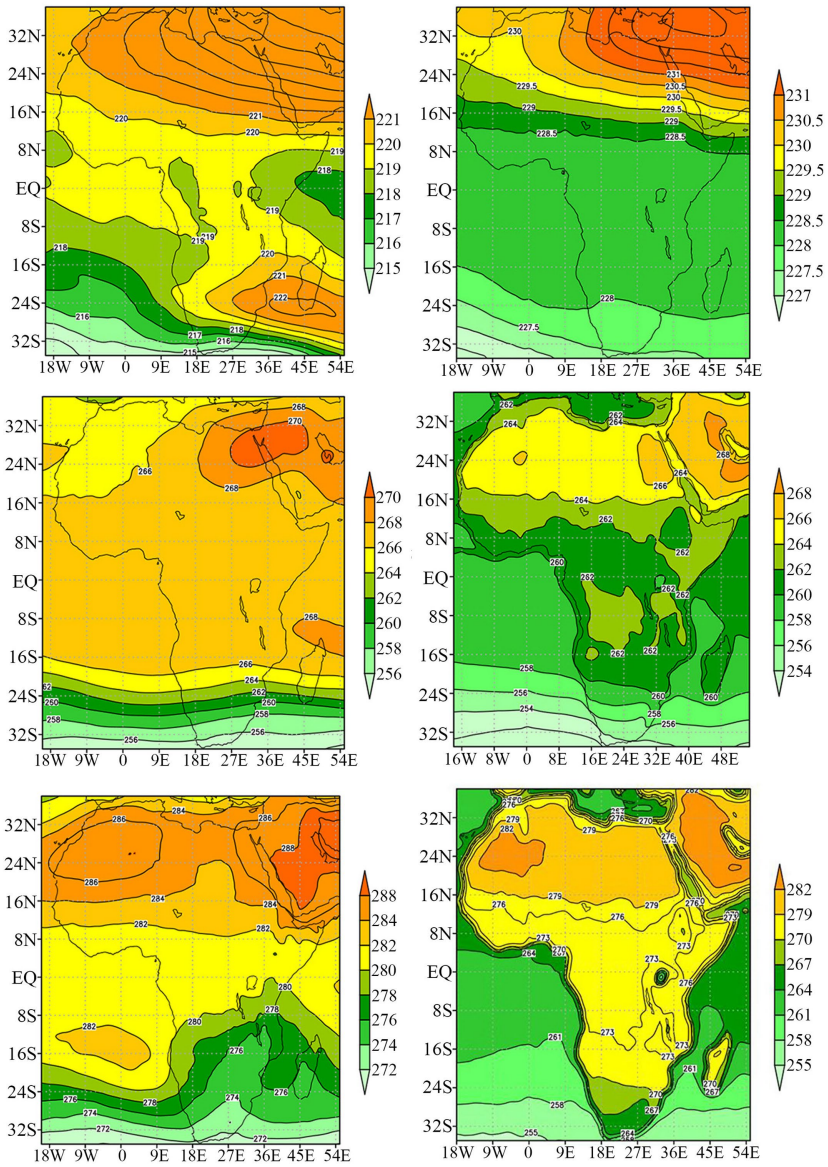

Figure 5. Spatial distribution of temperature at 100, 250, and 500 hPa for JRA-55 (left panels) and MERRA-2 (right panels) on rain season.

During the rainy season, atmospheric temperatures at all levels over Africa exhibit a gradual decrease from north to south, which may be attributed to the greater oceanic coverage in the southern part of the region. The AMSU-A data faithfully reproduce the characteristic pattern of higher temperatures in the north and lower temperatures in the south, and accurately capture the vertical structure over CAR, with colder temperatures in the upper troposphere and warmer temperatures in the lower troposphere. However, certain discrepancies exist between the two datasets. The spatial structure of brightness temperatures from AMSU-A appears notably smoother across all channels. Additionally, AMSU-A channel 9 (approximately 100 hPa) reveals a warm region in the southern part of the domain, which contrasts markedly with the ERA5 reanalysis. Similarly, the warm region in the southern do-

main identified in AMSU-A channel 5 (approximately 500 hPa) is shifted noticeably northward compared to that in ERA5.

Temperatures during the rainy season generally exhibit a gradual increase from south to north, which is opposite to the dry season, indicating that solar radiation exerts a dominant influence on the spatial distribution of temperature. Similarly, the AMSU-A dataset can well reproduce the atmospheric spatial structure in the reanalysis data, including the local high-temperature zone in the northeastern part of the region at 100 - 250 hPa. The characteristic that the high-temperature zone expands to the entire latitudinal belt at 500 hPa is also well captured. However, the land-sea contrast in the AMSU-A brightness temperature data is more pronounced, which may be an important factor responsible for its failure to adequately reproduce the low temperatures in the southeastern part of the region at 500 hPa (**Figure 4**).

There are also certain differences among different reanalysis datasets, as illustrated in **Figure 5**. At 100 hPa, the JRA-55 dataset shows an abnormally strong high-temperature zone in the southeastern part of the region. At 250 hPa, neither JRA-55 nor MERRA-2 exhibits an obvious zonal high-temperature zone near 10˚S. The temperature structure in this region from ERA5 is more similar to that from AMSU-A data.

4. Linear Temperature Trends (2000-2020)

Global warming has emerged as one of the most critical natural hazards confronting humanity (Please add some related references), and the rate of global warming serves as a fundamental metric for assessing its potential severity. Linear trends are frequently employed to quantify the pace of warming. The linear trend in temperature was calculated using ordinary least squares regression analysis of regionally averaged monthly temperature anomalies. All datasets indicate a statistically significant atmospheric warming over the Central African Republic (CAR) during the period of 2000-2020.

The linear trend results for atmospheric temperature at various levels indicate warming throughout the column from the lower stratosphere to the surface, suggesting that CAR is undergoing a comprehensive warming phase with an attendant increase in heat-related disaster risk. Notably, all datasets exhibit a consistent pattern of positive trends across all analyzed atmospheric levels, supporting the robustness of atmospheric warming over CAR irrespective of dataset selection.

Table 1. Linear trend (unit: K/10a) of different datasets.

Pressure level	AMSU-A	ERA5	JRA-55	MERRA-2
500 hpa	0.576	0.476	0.276	0.376
250 hPa	0.204	0.344	0.444	0.408
100 hPa	0.312	0.144	0.124	0.168

Concurrently, significant variations in warming rates are evident across different pressure levels. The maximum trends are observed at the 500 hPa level. AMSU-

A satellite observations reveal a temperature trend of 0.576 K/10a, while all reanalysis products show pronounced warming trends with generally lower magnitudes compared to the AMSU-A dataset. Among the reanalysis datasets, ERA5 demonstrates the closest agreement with AMSU-A, with a trend of 0.476 K/decade. At 100 hPa, the reanalysis products exhibit comparable warming trends, all slightly exceeding 0.1 K/10a; however, the AMSU-A warming rate reaches 0.312 K/10a. Conversely, at 250 hPa, the AMSU-A warming rate is markedly lower than that of the reanalysis products. Substantial discrepancies are also present among the reanalysis datasets themselves, with JRA-55 showing the strongest warming trend, though ERA5 again demonstrates the most consistent trend with the AMSU-A observations.

5. Vertical Synthesis of Linear Trends

In order to better understand the reasons for the discrepancies between satellite data and reanalysis products, as well as the discrepancies between reanalysis products themselves, vertical temperature profiles for the dry and rainy seasons were analyzed.

5.1. Dry Season

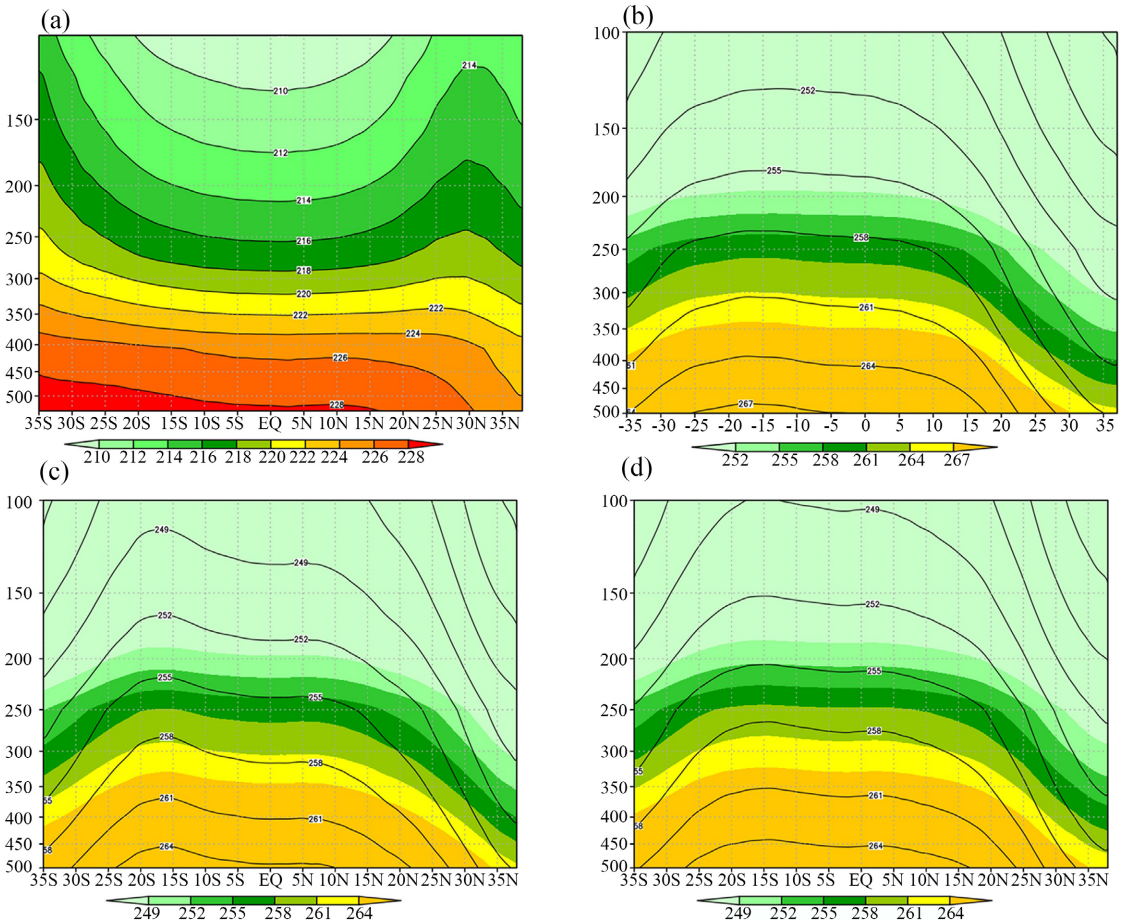

Figure 6. Vertical cross section for dry season (a) Satellite; (b) ERA5; (c) JRA-55; and (d) MERRA-2.

Figure 6 presents vertical cross-sections along the equator for different datasets during the dry season. All datasets exhibit a characteristic decrease in temperature with altitude, as well as a gradual decline in temperature from the equator toward higher latitudes on both sides. As the dry season coincides with winter in the Northern Hemisphere, the warm region is shifted predominantly toward the Southern Hemisphere, while temperatures in the Northern Hemisphere decrease rapidly with increasing latitude. The AMSU-A data faithfully reproduce the latitudinal temperature variations in the lower troposphere; however, at higher altitudes, the AMSU-A brightness temperatures display markedly different latitudinal patterns, even exhibiting a reversed structure with colder temperatures over the tropics and warmer temperatures on both sides. Examination of the AMSU-A weighting functions reveals that channel 9 brightness temperature is influenced not only by upper-tropospheric temperatures but also by lower-stratospheric temperatures. Given that the tropopause height is higher over the tropics than at higher latitudes, this vertical structural difference likely contributes to the higher brightness temperatures on the northern and southern flanks relative to the equatorial region at these altitudes.

5.2. Rainy Season

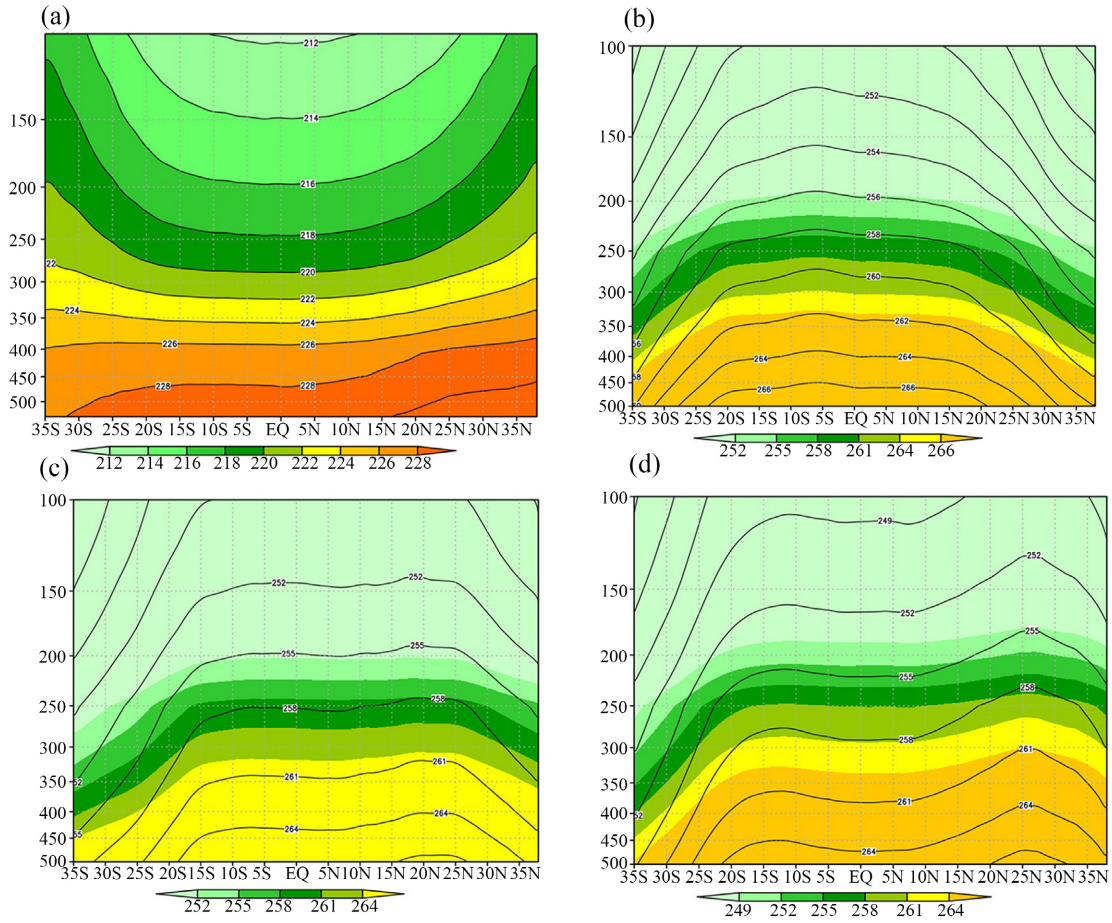

Figure 7. Vertical cross section for rainy season (a) Satellite; (b) ERA5; (c) JRA-55; and (d) MERRA-2.

During the rainy season, temperatures at all levels similarly decrease with altitude; however, the latitudinal temperature variation differs markedly from that of the dry season, as illustrated in Figure 7. Although the overall pattern remains one of warmer tropics and cooler extratropics, the low-level warm region shifts distinctly northward into the Northern Hemisphere due to the boreal summer timing of the rainy season. Additionally, a bimodal temperature structure emerges, with a temperature minimum occurring near 5˚N in the Northern Hemisphere—likely associated with the northward migration of the Intertropical Convergence Zone (ITCZ). The ITCZ maintains intense convective cloud bands year-round, where high albedo reflects solar radiation and evaporative cooling from precipitation creates a "cold trough" in temperature. This equatorial cloud-rain cooling, alternating with subtropical desert heat, produces the characteristic "cool center, warm flanks" bimodal structure of African summer temperatures. The AMSU-A data likewise capture the northward displacement of the low-level warm region and reproduce the corresponding bimodal structure in the lower troposphere. However, at higher altitudes, the AMSU-A brightness temperatures exhibit an increase with latitude toward both northern and southern flanks—a pattern distinctly different from the reanalysis products. This discrepancy likely contributes to the notable differences in climatic trends between AMSU-A brightness temperatures and reanalysis products at upper levels.

6. Nonlinear Temperature Trends

Previous studies have reported periods of slowdown in global or regional warming in the early 2010s (Kosaka & Xie, 2013; Medhaug et al., 2017), which were attributed to natural climate variability or ocean-atmosphere interactions. By isolating the residual low-frequency component after removing high-frequency components, EEMD represents a physically meaningful way of expressing changes in climate trends. Additionally, the EEMD method effectively filters noise, preventing individual extreme values from distorting the climate trend.

Figure 8 displays nonlinear temperature trends at 100, 250, and 500 hPa for Central Africa. The AMSU-A data exhibit pronounced nonlinear characteristics, whereas the reanalysis products demonstrate predominantly linear warming trends. Between 100 and 250 hPa, the AMSU-A data initially show rapid warming; however, around 2012, the warming rate decelerated markedly, with cooling even observed at 100 hPa. In contrast, the reanalysis products maintain a steady, gradual warming throughout the record. At 500 hPa, by comparison, the AMSU-A data first exhibit significant cooling, followed by rapid warming after approximately 2010, ultimately resulting in linear trends comparable to those of the reanalysis products. This suggests that different physical mechanisms may have dominated temperature changes around 2010. Discrepancies are also evident among the reanalysis products themselves: JRA-55 shows the weakest warming rate, while ERA5 exhibits substantially stronger warming than the other two reanalysis da-

tasets. Moreover, this accelerated warming in ERA5 becomes more pronounced with increasing altitude.

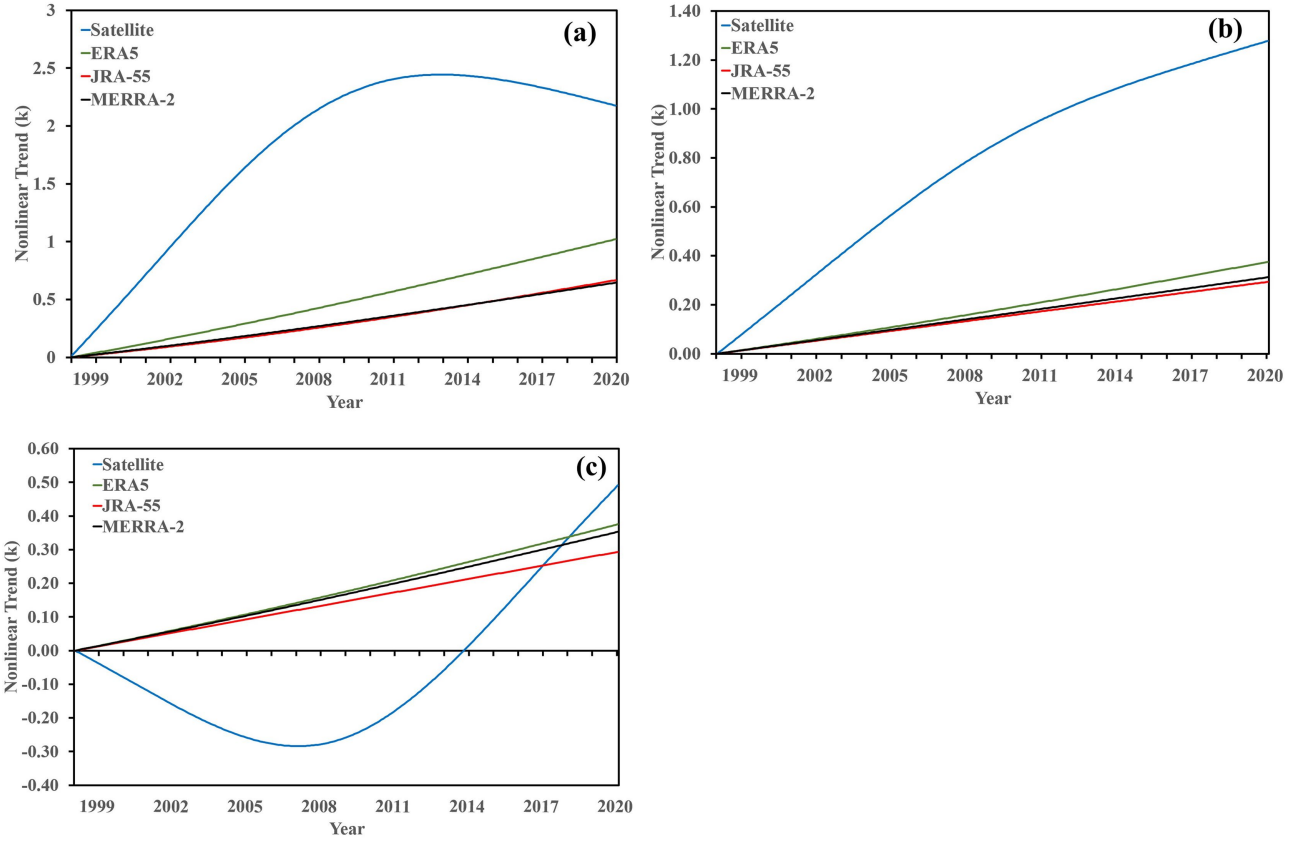

Figure 8. Nonlinear trend of regionally averaged atmospheric temperature at (a) 100, (b) 250, and (c) 500 hPa over Central Africa Republic.

The nonlinear characteristics in the warming behavior in CAR can be explained by earlier studies that reported the presence of variability in the rate of warming in the tropics, especially due to internal variability and ocean-atmosphere coupling mechanisms (Dosio et al., 2018; Harrington et al., 2016). The modulation observed at 500 hPa in the present study, where the satellite-derived nonlinear trend shows an initial cooling phase before accelerating warming after approximately 2008, is consistent with the so-called "global warming hiatus" documented in the literature during the early 2000s to mid-2010s. This temporary slowdown has been widely attributed to natural internal climate variability rather than a fundamental change in the Earth's energy balance.

In particular, Kosaka and Xie (2013) demonstrated that the global warming hiatus was largely driven by tropical Pacific sea surface cooling, itself a manifestation of natural decadal variability associated with the Pacific Decadal Oscillation (PDO). Similarly, (England et al., 2014) showed that an intensification of Pacific trade winds during this period enhanced subsurface ocean heat uptake, thereby suppressing surface warming temporarily. These ocean-atmosphere interactions,

which operate on interannual to decadal timescales, can modulate regional temperature trends in tropical Africa by altering large-scale circulation patterns and moisture fluxes (Kosaka & Xie, 2013; England et al., 2014).

While some have interpreted the slowdown in surface warming during the early 2000s as evidence for reduced climate sensitivity, other studies argue that internal variability merely masks the long-term warming trend rather than indicating a weakening of the greenhouse effect. England et al. (2014) specifically emphasized that rapid warming is expected to resume once the anomalous wind trends abate, and subsequent observations have confirmed this recovery. The nonlinear EEMD trends obtained in the present study at 250 and 100 hPa, which show a near-monotonic acceleration throughout 1999-2020, further support this interpretation: while mid-tropospheric levels are more sensitive to decadal variability, upper-tropospheric and lower-stratospheric warming continued uninterrupted, consistent with the sustained increase in greenhouse gas concentrations.

Taken together, these findings underscore the importance of applying nonlinear analytical methods such as EEMD when assessing climate trends in data-sparse tropical regions like CAR. Linear regression alone would obscure the decadal-scale fluctuations revealed here, potentially leading to an underestimation or misinterpretation of the true warming signal (Medhaug et al., 2017).

7. Discussion

The results show that the AMSU-A and the three modern reanalysis datasets (ERA5, JRA-55, and MERRA-2) consistently show a warming trend in the Central African Republic from 2000 to 2020. The consistency in the sign of the trend for all datasets is strong evidence that the detected trend is real.

The consistency between the AMSU-A datasets and reanalysis datasets is strong evidence that modern reanalysis datasets are able to represent the evolution of the temperature in the atmosphere on a large scale in Central Africa, especially for temperature in the mid-troposphere and low-stratosphere layers (500 and 250 hPa). In the nonlinear trend analysis, the AMSU-A observations display markedly nonlinear trend behavior, in stark contrast to the quasi-linear warming trajectories evident in all reanalysis datasets. As AMSU-A constitutes a direct observational record, this divergence suggests potential over-smoothing of temperature trends in the reanalysis products.

Among the reanalysis data products examined in this study, ERA5 shows the highest overall consistency with satellite data, especially at the 250 and 500 hPa level. JRA-55 and MERRA-2 show similar features in the warming trend but with slightly weaker trend amplitudes and smoother nonlinear components, This further suggests that, among the reanalysis products examined, ERA5 is comparatively better suited for climatological investigations over the CAR region. The largest satellite-reanalysis difference is seen at the 250 hPa level and can be explained by the action of two different physical effects. First, the weighting function of AMSU-A Channel 7 has a wide quasi-Gaussian shape with contributions to the

signal from ~150 - 400 hPa pressure levels. This level of vertical smoothing of the signal, combining the upper troposphere and lower stratosphere, cannot be captured by the single pressure level of the reanalysis data. Second, the pressure level of 250 hPa is close to the tropical tropopause layer (TTL; ~150 - 200 hPa), in which the height of the tropopause has strong inter-annual variability associated with QBO and ENSO. When the tropopause height changes with altitude, the cold-point temperature seen by Channel 7 changes dramatically, and this signal is not captured in the reanalysis data.

8. Conclusion

This paper presents a detailed assessment of temperature variability and trends in the atmosphere over the Central African Republic (CAR) using AMSU-A satellite data and three recent reanalysis datasets: ERA5, JRA-55, and MERRA-2, for the period from 2000 to 2020.

All datasets show statistically significant warming trends in the atmosphere, specifically in the low and mid-troposphere. Consistency in sign among independent satellite data and reanalysis datasets is strong evidence that temperatures in the atmosphere over CAR have been rising, as seen in other tropical and global climate trends (Essa et al., 2022; Ladstädter et al., 2023; Santer et al., 2017). Although the linear warming trends across different datasets exhibit a certain degree of similarity, the AMSU-A data display more pronounced nonlinear trend characteristics, whereas the reanalysis products are dominated by approximately linear warming patterns. As far as vertical agreement is concerned, the most consistent results of all four datasets are found in 500 hPa height, followed by 100 hPa; the largest inter-product discrepancies are found in 250 hPa due to tropopause layer variability and AMSU-A channel-7 weighting function effects.

The results from this study emphasize the need for the complementarity of satellite data and high-quality reanalysis data in climate monitoring in the data-sparse tropics. Though reanalysis data are able to capture the large-scale atmospheric temperature variability well, satellite data are still necessary for capturing the nonlinear variability. Further improvement in the *in situ* meteorological observation network and the simulation of land-atmosphere feedback processes in atmospheric models is also a prerequisite for enhancing the capability in climate risk assessment and adaptation in Central Africa.

Conflicts of Interest

The authors declare no conflicts of interest regarding the publication of this paper.

References

Abaje, I., Sawa, B., Iguisi, E., & Ibrahim, A. (2016). Impacts of Climate Change and Adaptation Strategies in Rural Communities of Kaduna State, Nigeria. *Ethiopian Journal of Environmental Studies and Management, 9,* 97-108. https://doi.org/10.4314/ejesm.v9i1.9

Adler, R. F., Gu, G., Sapiano, M., Wang, J., & Huffman, G. J. (2017). Global Precipitation:

Means, Variations and Trends during the Satellite Era (1979-2014). *Surveys in Geophysics, 38,* 679-699. https://doi.org/10.1007/s10712-017-9416-4

Almazroui, M., Saeed, F., Saeed, S., Ismail, M., Ehsan, M. A., Islam, M. N. et al. (2021). Projected Changes in Climate Extremes Using CMIP6 Simulations over SREX Regions. *Earth Systems and Environment, 5,* 481-497. https://doi.org/10.1007/s41748-021-00250-5

Dinku, T. (2019). Challenges with Availability and Quality of Climate Data in Africa. In A. M. Melesse, W. Abtew, & G. Senay (Eds.), *Extreme Hydrology and Climate Variability* (pp. 71-80). Elsevier. https://doi.org/10.1016/b978-0-12-815998-9.00007-5

Dosio, A., Jury, M. W., Almazroui, M., Ashfaq, M., Diallo, I., Engelbrecht, F. A. et al. (2021). Projected Future Daily Characteristics of African Precipitation Based on Global (CMIP5, CMIP6) and Regional (CORDEX, CORDEX-CORE) Climate Models. *Climate Dynamics, 57,* 3135-3158. https://doi.org/10.1007/s00382-021-05859-w

Dosio, A., Mentaschi, L., Fischer, E. M., & Wyser, K. (2018). Extreme Heat Waves under 1.5 °C and 2 °C Global Warming. *Environmental Research Letters, 13,* Article 054006. https://doi.org/10.1088/1748-9326/aab827

England, M. H., McGregor, S., Spence, P., Meehl, G. A., Timmermann, A., Cai, W. et al. (2014). Recent Intensification of Wind-Driven Circulation in the Pacific and the Ongoing Warming Hiatus. *Nature Climate Change, 4,* 222-227. https://doi.org/10.1038/nclimate2106

Essa, Y. H., Cagnazzo, C., Madonna, F., Cristofanelli, P., Yang, C., Serva, F. et al. (2022). Intercomparison of Atmospheric Upper-Air Temperature from Recent Global Reanalysis Datasets. *Frontiers in Earth Science, 10,* Article ID: 935139. https://doi.org/10.3389/feart.2022.935139

Ferraro, R. R., Nelson, B. R., Smith, T., & Prat, O. P. (2018). The AMSU-Based Hydrological Bundle Climate Data Record—Description and Comparison with Other Data Sets. *Remote Sensing, 10,* 1640. https://doi.org/10.3390/rs10101640

Fotso-Nguemo, T. C., Vondou, D. A., Diallo, I., Diedhiou, A., Weber, T., Tanessong, R. S. et al. (2022). Potential Impact of 1.5, 2 and 3 °C Global Warming Levels on Heat and Discomfort Indices Changes over Central Africa. *Science of The Total Environment, 804,* Article 150099. https://doi.org/10.1016/j.scitotenv.2021.150099

Funk, C., Shukla, S., Thiaw, W. M., Rowland, J., Hoell, A., McNally, A. et al. (2019). Recognizing the Famine Early Warning Systems Network: Over 30 Years of Drought Early Warning Science Advances and Partnerships Promoting Global Food Security. *Bulletin of the American Meteorological Society, 100,* 1011-1027. https://doi.org/10.1175/bams-d-17-0233.1

Gelaro, R., McCarty, W., Suárez, M. J., Todling, R., Molod, A., Takacs, L., Randles, C. A., Darmenov, A., Bosilovich, M. G., Reichle, R., Wargan, K., Coy, L., Cullather, R., Draper, C., Akella, S., Buchard, V., Conaty, A., da Silva, A. M., Gu, W. et al. (2017). *The Modern-Era Retrospective Analysis for Research and Applications, Version 2 (MERRA-2).* https://doi.org/10.1175/JCLI-D-16-0758.1

Harrington, L. J., Frame, D. J., Fischer, E. M., Hawkins, E., Joshi, M., & Jones, C. D. (2016). Poorest Countries Experience Earlier Anthropogenic Emergence of Daily Temperature Extremes. *Environmental Research Letters, 11,* Article 055007. https://doi.org/10.1088/1748-9326/11/5/055007

Hersbach, H., Bell, B., Berrisford, P., Hirahara, S., Horányi, A., Muñoz-Sabater, J. et al. (2020). The ERA5 Global Reanalysis. *Quarterly Journal of the Royal Meteorological Society, 146,* 1999-2049. https://doi.org/10.1002/qj.3803

Hua, W., Zhou, L., Nicholson, S. E., Chen, H., & Qin, M. (2019). Assessing Reanalysis Data

for Understanding Rainfall Climatology and Variability over Central Equatorial Africa. *Climate Dynamics, 53,* 651-669. https://doi.org/10.1007/s00382-018-04604-0

Kobayashi, S., Ota, Y., Harada, Y., Ebita, A., Moriya, M., Onoda, H. et al. (2015). The JRA-55 Reanalysis: General Specifications and Basic Characteristics. *Journal of the Meteorological Society of Japan. Ser. II, 93,* 5-48. https://doi.org/10.2151/jmsj.2015-001

Kosaka, Y., & Xie, S. (2013). Recent Global-Warming Hiatus Tied to Equatorial Pacific Surface Cooling. *Nature, 501,* 403-407. https://doi.org/10.1038/nature12534

Ladstädter, F., Steiner, A. K., & Gleisner, H. (2023). Resolving the 21st Century Temperature Trends of the Upper Troposphere-Lower Stratosphere with Satellite Observations. *Scientific Reports, 13,* Article No. 1306. https://doi.org/10.1038/s41598-023-28222-x

Legg, S. (2021). IPCC, 2021: Climate Change 2021—The Physical Science Basis. *Interaction, 49,* 44-45.

Mbétid-Bessane, E., Djondang, K., Havard, M., & Kadékoy-Tigagué, D. (2010). Impacts des changements de politique dans un contexte de crise mondialisée sur les acteurs des filières cotonnières d'Afrique centrale. *Cahiers Agricultures, 19,* 21-27. https://doi.org/10.1684/agr.2009.0339

Mears, C. A., & Wentz, F. J. (2009). Construction of the RSS V3.2 Lower-Tropospheric Temperature Dataset from the MSU and AMSU Microwave Sounders. *Journal of Atmospheric and Oceanic Technology, 26,* 1493-1509. https://doi.org/10.1175/2009jtecha1237.1

Medhaug, I., Stolpe, M. B., Fischer, E. M., & Knutti, R. (2017). Reconciling Controversies about the 'Global Warming Hiatus'. *Nature, 545,* 41-47. https://doi.org/10.1038/nature22315

Mudelsee, M. (2019). Trend Analysis of Climate Time Series: A Review of Methods. *Earth-Science Reviews, 190,* 310-322. https://doi.org/10.1016/j.earscirev.2018.12.005

Nangombe, S. S., Zhou, T., Zhang, W., Zou, L., & Li, D. (2019). High-Temperature Extreme Events over Africa under 1.5 and 2˚C of Global Warming. *Journal of Geophysical Research: Atmospheres, 124,* 4413-4428. https://doi.org/10.1029/2018jd029747

Ndiaye, P. M., Bodian, A., Diop, L., Deme, A., Dezetter, A., Djaman, K. et al. (2020). Trend and Sensitivity Analysis of Reference Evapotranspiration in the Senegal River Basin Using NASA Meteorological Data. *Water, 12,* Article 1957. https://doi.org/10.3390/w12071957

Ngoma, H., Pelletier, J., Mulenga, B. P., & Subakanya, M. (2021). Climate-Smart Agriculture, Cropland Expansion and Deforestation in Zambia: Linkages, Processes and Drivers. *Land Use Policy, 107,* Article 105482. https://doi.org/10.1016/j.landusepol.2021.105482

Nzoumbou-Boko, R., Velut, G., Imboumy-Limoukou, R., Manirakiza, A., & Lekana-Douki, J. (2022). Malaria Research in the Central African Republic from 1987 to 2020: An Overview. *Tropical Medicine and Health, 50,* Article No. 70. https://doi.org/10.1186/s41182-022-00446-z

Ogunrinde, A. T., Oguntunde, P. G., Akinwumiju, A. S., & Fasinmirin, J. T. (2019). Analysis of Recent Changes in Rainfall and Drought Indices in Nigeria, 1981-2015. *Hydrological Sciences Journal, 64,* 1755-1768. https://doi.org/10.1080/02626667.2019.1673396

Qin, Z., & Zou, X. (2023). Modulation Effect of the Annual Cycle on Interdecadal Warming Trends over the Tibetan Plateau during 1998-2020. *Journal of Climate, 36,* 2917-2931. https://doi.org/10.1175/jcli-d-22-0517.1

Quénol, H. (2011). Observation et modélisation spatiale du climat aux échelles fines dans un contexte de changement climatique. Université Rennes 2.

Rohde, R., Muller, R., Jacobsen, R., Perlmutter, S., & Mosher, S. (2016). Berkeley Earth Temperature Averaging Process. *Geoinformatics & Geostatistics: An Overview, 1.*

https://doi.org/10.4172/2327-4581.1000103

Saber, M., Koroma, A., Posite, R. V., LY, A., Tejan Bah, A. M., Abdulai, A. et al. (2025). A Comprehensive Review of Climate Change Adaptation and Disaster Risk Reduction in Africa. *Journal of Water and Climate Change, 16,* 1831-1862. https://doi.org/10.2166/wcc.2025.741

Santer, B. D., Mears, C., Doutriaux, C., Caldwell, P., Gleckler, P. J., Wigley, T. M. L., Solomon, S. et al. (2017). Separating Signal and Noise in Atmospheric Temperature Changes: The importance of Timescale. *Journal of Geophysical Research Atmospheres, 116,* D22.

Sylla, M. B., Nikiema, P. M., Gibba, P., Kebe, I., & Klutse, N. A. B. (2016). Climate Change over West Africa: Recent Trends and Future Projections. In J. A. Yaro, & J. Hesselberg (Eds.), *Adaptation to Climate Change and Variability in Rural West Africa* (pp. 25-40). Springer International Publishing. https://doi.org/10.1007/978-3-319-31499-0_3

Vincent, L. A., Wang, X. L., Milewska, E. J., Wan, H., Yang, F., & Swail, V. (2012). A Second Generation of Homogenized Canadian Monthly Surface Air Temperature for Climate Trend Analysis. *Journal of Geophysical Research: Atmospheres, 117,* D18110. https://doi.org/10.1029/2012jd017859

Washington, S., Karlaftis, M. G., Mannering, F., & Anastasopoulos, P. (2020). *Statistical and Econometric Methods for Transportation Data Analysis.* https://doi.org/10.1201/9780429244018

Weng, K. C., Castilho, P. C., Morrissette, J. M., Landeira-Fernandez, A. M., Holts, D. B., Schallert, R. J. et al. (2005). Satellite Tagging and Cardiac Physiology Reveal Niche Expansion in Salmon Sharks. *Science, 310,* 104-106. https://doi.org/10.1126/science.1114616

Wu, Z., Huang, N. E., & Chen, X. (2011). The Multi-Dimensional Ensemble Empirical Mode Decomposition Method. *Advances in Adaptive Data Analysis. (World), 1,* 339-372.